UNIVERSITY OF WEST LONDON
The Career University

UWL REPOSITORY

repository.uwl.ac.uk

Laboratory investigations for the electromagnetic characterization of railway ballast through GPR

Tosti, Fabio ORCID: https://orcid.org/0000-0003-0291-9937, Benedetto, Andrea, Calvi, Alessandro and Bianchini Ciampoli, Luca (2016) Laboratory investigations for the electromagnetic characterization of railway ballast through GPR. In: 16th International Conference on Ground Penetrating Radar (GPR 2016), 13-16 June 2016, Hong Kong.

http://dx.doi.org/10.1109/ICGPR.2016.7572605

This is the Accepted Version of the final output.

UWL repository link: https://repository.uwl.ac.uk/id/eprint/2235/

Alternative formats: If you require this document in an alternative format, please contact: open.research@uwl.ac.uk

Copyright:

Copyright and moral rights for the publications made accessible in the public portal are retained by the authors and/or other copyright owners and it is a condition of accessing publications that users recognise and abide by the legal requirements associated with these rights.

Take down policy: If you believe that this document breaches copyright, please contact us at open.research@uwl.ac.uk providing details, and we will remove access to the work immediately and investigate your claim.

Laboratory Investigations for the Electromagnetic Characterization of Railway Ballast through GPR

F. Tosti
School of Computing and Engineering, University of West London (UWL)
St Mary's Road, Ealing, W5 5RF, London, UK
Fabio.Tosti@uwl.ac.uk

A. Benedetto, A. Calvi, L. Bianchini Ciampoli
Department of Engineering, Roma Tre University
Via Vito Volterra 62, 00146, Rome, Italy
andrea.benedetto@uniroma3.it,
alessandro.calvi@uniroma3.it,
luca.bianchiniciampoli@uniroma3.it

***Abstract*— Ballast material typically employed in rail track bed construction has been herein physically and electromagnetically characterized. Several ground-penetrating radar (GPR) tests have been carried out in a laboratory environment, wherein a proper set-up was realized. Four GPR systems comprising five different central frequencies of investigation have been used for the measurements. The impacts brought to the values of relative dielectric permittivity by the combination of several parameters, namely, i) radar systems, ii) frequencies of investigation, iii) scenarios of ballast stones arrangement, and iv) methods of dielectric permittivity estimate, have been here analyzed. The results have proved the sensitivity of the antenna frequencies and radar systems here employed towards some critical factors.**

***Index Terms*—GPR, ground-penetrating radar, railway ballast, frequency of investigation, dielectric permittivity.**

I. Introduction

Railway ballast is a very important component of a rail infrastructure as it must perform several key functions such as lowering the stresses applied to the weaker interfaces, resisting to the vertical, lateral, and longitudinal forces applied to the sleepers for maintaining the track position, and providing proper drainage of water from the track structure [1]. With regard to its mineralogy, it is a uniformly graded coarse aggregate made of crushed hard rock or, sometimes, crushed gravel material, where smaller mineral particles have been sieved away. It is placed between and immediately underneath the railway ties.

Sub-ballast is instead a sand- or gravel-made material, which improves the drainage properties and the distribution of the applied train loading over the subgrade. Generally speaking, the ballast and sub-ballast system is considered as a granular layer with a design thickness ranging between 0.45 m and 0.75 m, and it can be frequently found in rehabilitated and newly constructed lines, while old rail infrastructures mostly consist of only one ballast layer above the subgrade [2]. In addition, a filtering layer, generally consisting of a concrete slab or a geotextile, is arranged at the sub-ballast (if any) - subgrade interface in new railroads, while in old railways the ballast or the sub-ballast layer lies directly over the subgrade.

One of the major problems affecting ballast is related to the formation of fouling, which is a contamination of fine material and metal dust filling the voids within the ballast grains. Fouling can be basically attributed to three main factors; namely, i) the abrasion of the ballast grains due to the contact points between the stones, ii) the loss of metal dust in the contact between train wheels and rails, and iii) the capillary rise of fine materials due to groundwater presence in the subsurface. The detection of ballast fouling is of primary importance, since when it reaches a specific content, the structural integrity and the drainage ability of the ballast system can be affected. This implies track instability, which in turn may lead to train derailments. Therefore, it is very important to provide an early detection of ballast fouling in terms of track bed stability, safety and efficient renewal planning.

In line with the above, railway engineering increasingly needs to use even more time-efficient and cost-effective technologies capable of minimizing the time and cost of interventions. According to this, ground-penetrating radar (GPR) seems to be the most promising technique for non-destructively and rapidly detecting railroad substructures. Such non-destructive testing (NDT) technology has proven to be one of the most reliable geophysical inspection tools spanning a wide range of application areas from planetary explorations [3], to civil and environmental engineering [4], from geology [5] and archaeology [6], to forensics and public safety [7]. By using GPR it is possible to detect the main physical properties of the subsurface through the transmission/reception of electromagnetic (EM) waves in a given frequency band [8]. Within the transport engineering area, several applications can be found: i) in pavement engineering [9], for both bound [10]−[13] and unbound [14]−[16] flexible pavement layers, concrete pavements [17], and subgrade soils [18], [19]; ii) in airfield engineering [20]; and iii) applications focused on the monitoring of critical infrastructures, such as bridges [21], [22] and tunnels [23].

Within the area of railway engineering, the use of GPR has increased over the past 25 years, and it has seen several attempts at setting the proper center frequency of investigation. According to [24], the first attempt at using GPR in railway engineering can be traced back to 1985 [25], and involved the use of 500 MHz ground-coupled antennas mounted between the rails. Many difficulties in the interpretation of the results were experienced here due to the low resolution of the images produced. Higher frequency air-coupled antennas, mostly of 1000 MHz [26], [27], have instead been widely used in the following years. More recently, more resolute horn antennas with a central frequency of 2000 MHz are also being used and frequency-based approaches have been developed accordingly [2], [28].

Several landmark studies on the characterization of the ballast-sub-ballast material have been carried out over the past years. In [1], a number of laboratory experiments were undertaken to characterize the dielectric properties of dry and wet railway track ballast in both clean and spent conditions. It was argued that best results were achieved using low-frequency antennas. [29] shows how the mineralogy of the ballast stones is a necessary but not sufficient property for explaining their EM behavior, due to its dependence on the material shape and placement within the track beds. A thorough review of the EM characterization of railway ballast can be found in [30].

II. METHODOLOGY AND OBJECTIVE

In this paper, the EM behavior of a clean basalt railway ballast has been analyzed in dry conditions using several GPR instruments, in both ground-coupled and air coupled configurations, with different central frequencies of investigation spanning from 600 MHz to 2000 MHz. Basically, the signals collected have been first processed and all the useless information filtered out from the raw signals. Then, the relative dielectric permittivity of the air-ballast system has been evaluated by means of an estimate of the wave propagation velocity within the medium, e.g., [31]. In the case of air-coupled antenna systems, the surface reflection method (SRM) [32] has been also employed for retrieving the permittivity of the medium. The laboratory experiments were undertaken in a methacrylate tank wherein the ballast was filled and emptied several times, such that different scenarios in terms of the arrangement of stones were performed.

The specific objective of this work is therefore aimed at analyzing the EM response of this material as a function of the frequency of investigation, the system configuration, the arrangement of the ballast stones, and the permittivity estimate method.

III. DATA PROCESSING AND THEORETICAL BACKGROUND

In this Section, an overview of the two main steps performed on the raw radar signals collected will be given; namely, the signal processing techniques, and the methods employed for the estimation of the relative dielectric permittivity.

A. Data Processing Scheme

A four-step data processing scheme, namely, i) time-zero correction, ii) signal stacking, iii) band-pass filtering, and iv) zero-offset removal, was applied to the raw GPR signals in line with [33], [34]. The above steps were performed in both the time (i.e., steps i), ii), and iv)) and the frequency domain (i.e., step iii)). Fig. 1 represents the processing scheme undertaken and the relevant signals achieved at each of the aforementioned steps for one of the radar systems employed in this study.

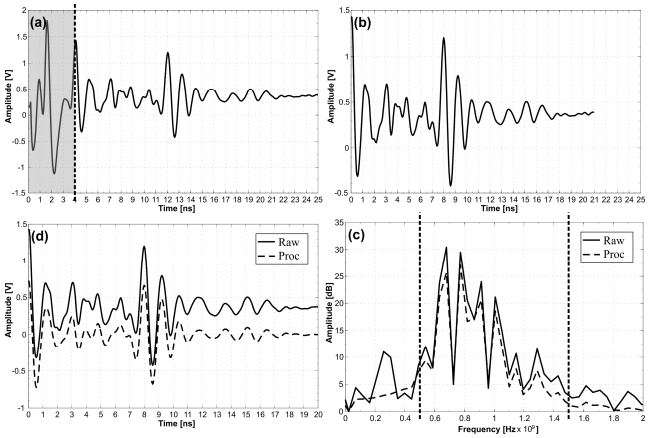

Fig. 1. Data processing scheme and relevant GPR signals achieved after time-zero correction (a), signal stacking (b), band-pass filtering (c), and zero-offset removal (d) for the data collected with a 1 GHz horn radar system

Firstly, a time-zero correction (Fig. 1a) was applied to filter out from the whole received signal all the reflections coming from within the radar apparatus, and also to set the zero position at the first largest amplitude of the direct wave (i.e., the interface between the air and the railway ballast surface). In the next step, the signal was averaged (stacked) over 100 traces (Fig. 1b), in line with the overall recommendations given in [35]. Indeed, by stacking several traces collected from the same position, the contributions from the target medium increase, whereas the random noise tends to reduce. Subsequently, a band-pass filtering (Fig. 1c) was performed on the signal spectrum in the frequency domain after applying a Fast Fourier Transform (FFT) to the time-domain signal processed at the previous step. A pass bandwidth of 1.5 times the central frequency was considered for all the antennas used in this study [36]. Finally, a zero-offset removal was applied after having back converted the signal from the frequency to the time domain (Fig. 1d), such that A-scan signals with a mean equal to zero have been achieved.

B. Dielectric Permittivity Estimate

The relative dielectric permittivity ε_r of the multi-phase system consisting of air voids and ballast stones (from now on referred to as "ballast system") was retrieved by means of an estimate of the wave propagation velocity v throughout the known thickness h of the material, which filled up the whole volume of the tank. In more detail, by measuring the time

delay Δt between the signal pulse reflections relative to the surface and the foundation of the ballast system, v can be estimated as $v = 2h/\Delta t$. The relative dielectric permittivity ε_r can be then calculated by changing the above expression of v into the following relationship:

$$\varepsilon_r=(c/v)^2 \quad (1)$$

where c is the speed of light in free space. Such a method (from now on referred to as "time-domain signal picking" (TDSP)) was used for the permittivity estimates on the data collected with both the radar systems and available frequencies .

Concerning the data arising from the use of the horn systems, the permittivity of the ballast system was also assessed by means of the SRM approach [32], as follows:

$$\varepsilon_r=\left(\frac{1+A_{\mathrm{PEC}}/A_{\mathrm{m}}}{1-A_{\mathrm{PEC}}/A_{\mathrm{m}}}\right)^2 \quad (2)$$

where A_0 is the maximum absolute signal amplitude reflected at the interface of the air/ballast surface, and A_{PEC} is the maximum absolute amplitude reflected by a metal plate placed at the bottom of the ballast and larger than the GPR footprint, which acts as a perfect electric conductor (PEC).

IV. Experimental Framework

A. Experimental Design

The experimental design is aimed at characterizing the clean basalt ballast used herein in dry conditions by analyzing its EM behavior for a combination of several parameters; namely, i) radar systems, ii) frequencies of investigation, iii) scenarios of ballast stone arrangements, and iv) methods of dielectric permittivity estimation. Preliminary analyses were undertaken with all the GPR systems available to ensure that the investigated domain might be assumed to be horizontally infinite, thereby allowing the manufacture of a tank within which border effects can be neglected.

B. Tools and Equipment

The experimental tests were carried out using ground-coupled and air-coupled pulsed radar systems [36], all manufactured by IDS Ingegneria dei Sistemi S.p.A. (Fig. 2). The RIS 99-MF Multi Frequency Array Radar-System, allowed the collection of data with 600 MHz and 1600 MHz central frequency antennas. Such a system is capable of performing measurements with four channels, i.e., two mono-static and two bi-static. In this study, the 600 MHz and 1600 MHz mono-static signals, collected within a time window of 40 ns, are considered. Moreover, three air-coupled devices with central frequencies of 1000 MHz (RIS Hi-Pave HR1 1000), and 2000 MHz (RIS Hi-Pave HR1 2000 and 2000 NA) were used. Time windows of 25 ns and 15 ns were set for, respectively, the 1000 MHz and the 2000 MHz systems. With regard to the latter frequency, a depowered version of the horn antenna for the North-American (NA) market was here employed. The railway ballast was investigated within a square-base methacrylate tank, with an outer base side and height of, respectively, 1.55 m and 0.55 m (Fig. 3), and inner dimensions of 1.47 m for both the base sides and 0.476 m for the height. The tank was laid above a 2 m × 2 m copper sheet PEC, which allowed for complete reflection of the waves propagating through the investigated material.

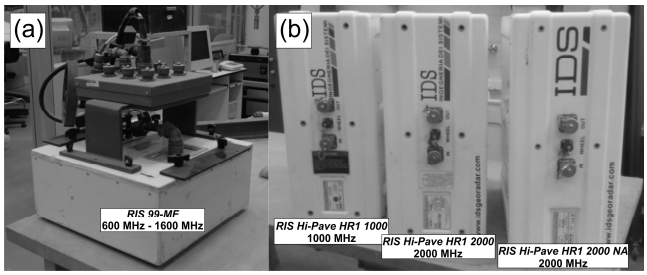

Fig. 2. GPR instruments used for testing: ground-coupled multi-channel radar system (a), and air-coupled horn radar systems (b)

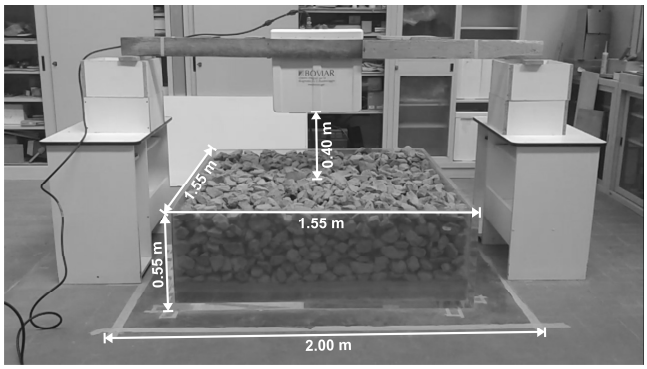

Fig. 3. Setup for a laboratory measurement performed with an air-coupled radar system

C. Materials and Laboratory Testing

Basalt stones, typically employed for the construction of railway ballast structures [37], were used for testing. Table 1 summarizes the main geometrical, physical, and performance properties of the material investigated.

TABLE I. Main Geometrical, Physical, and Performance Properties of the Railway Ballast Stones Used for the Laboratory Tests

Geometrical, physical, performance property	Regulation	Reference unit	Value
Grain size	EN 933-1: 2012 [38]	% passing vs. sieve size (mm): 80 -63 -50 -40 - 31.5 – 22.4	100 – 100 -79.9 – 30.6 – 1.2 – 0.3
Fine particles content	EN 933-1:2012 [38]	% passing vs. sieve size (mm): 0.063	0.5
Resistance to fragmentation	EN 1097-2:2010 [39]	% L.A. coeff.	20.0
Moisture	CEN ISO/TS 17892-1:2005 [40]	%	0.2
Particle density	EN 1097-6:2013 [41]	g/cm^3	2.8
Percentage of voids	EN 1097-3:1998 [42]	%	41.0

Overall, 1 test was carried out with the ground-coupled radar system, which allowed the collection of 100 traces for each relevant frequency. Calibration measurements complying with [35] were developed for the air-coupled radar systems, thereby allowing a reference distance of 0.40 m between the base of the GPR apparatus and the PEC to be set. That distance was therefore maintained between the base of each air-coupled apparatus and the surface of the ballast system. Three scenarios of ballast stone arrangement were reproduced by filling up and emptying the tank, and measurements were carried out accordingly for each of the three air-coupled systems, such that 9 tests were developed.

V. Results And Short Discussion

A. Ground-Coupled Antenna Systems

In Fig. 4 the relative dielectric permittivity estimates of the ballast system, performed in line with Eq. (1), are represented. The TDSP method was applied here to both the raw and the processed signals from the 600MHz-600MHz and the 1600MHz-1600MHz mono-static channels.

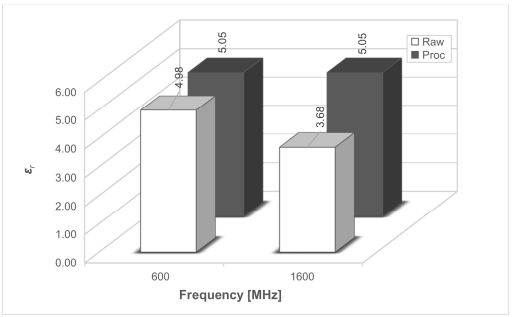

Fig. 4. Relative dielectric permittivity estimates (raw and processed) for the 600 MHz and 1600 MHz central-frequency acquisitions

The main mismatch between raw and processed data is in the case of the higher frequency, where the incidences of residuals (i.e., the percentage ratio of the difference between raw and processed dielectric permittivity values, and the corresponding raw value of dielectrics) are equal to 37.18% and 1.39% for, respectively, the 1600 MHz and the 600 MHz central frequencies. The application of the data processing scheme led to identical values of ε_r. It is nevertheless worth noting that the processed values of permittivity are 1.0÷1.5 units higher than those of similar materials from the literature, i.e., [1], [28]-[29], thereby indicating that such an antenna type is not well-suited for characterization purposes and for measuring the permittivity of rail ballast. A possible reason may be related to the effects of ringing, due to the difficulty of keeping the radar apparatus within one-eighth of the two antennas' wavelengths above the rough surface of the ballast [43]. In such a case, the low directivity of the antennas make these GPR systems more sensitive to the coarse grain size of the material and to edge effects, which may both affect the value of permittivity [44].

B. Air-Coupled Antenna Systems

Fig. 5 shows the permittivity values assessed for the combination of each of the three air-coupled systems and the

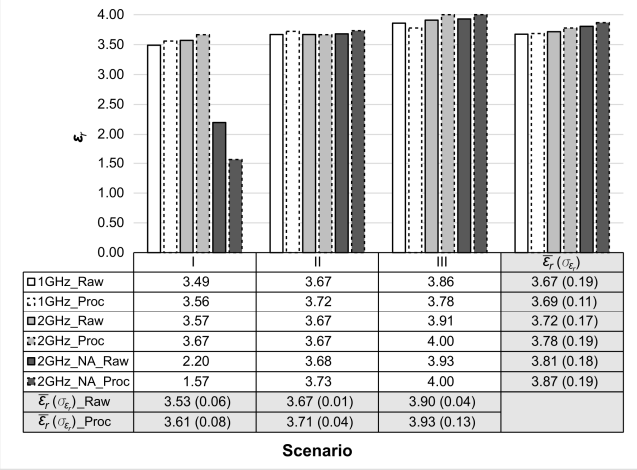

	I	II	III	$\overline{\varepsilon_r}\,(\sigma_{\varepsilon_r})$
1GHz_Raw	3.49	3.67	3.86	3.67 (0.19)
1GHz_Proc	3.56	3.72	3.78	3.69 (0.11)
2GHz_Raw	3.57	3.67	3.91	3.72 (0.17)
2GHz_Proc	3.67	3.67	4.00	3.78 (0.19)
2GHz_NA_Raw	2.20	3.68	3.93	3.81 (0.18)
2GHz_NA_Proc	1.57	3.73	4.00	3.87 (0.19)
$\overline{\varepsilon_r}\,(\sigma_{\varepsilon_r})$_Raw	3.53 (0.06)	3.67 (0.01)	3.90 (0.04)	
$\overline{\varepsilon_r}\,(\sigma_{\varepsilon_r})$_Proc	3.61 (0.08)	3.71 (0.04)	3.93 (0.13)	

Fig. 5. Relative dielectric permittivity estimates (raw and processed) for the 1000 MHz, 2000 MHz, and 2000 MHz (NA) central-frequency acquisitions

three scenarios of ballast system. Such values are in line with those provided in the literature, with the exception of the raw and processed dielectrics of the first scenario with the 2000 MHz (NA) antenna, which have been excluded from the statistics as outliers. Lower peaks of variability of the permittivity have been achieved for the whole set of frequencies within each scenario (i.e., $\sigma_{\varepsilon_r} = 0.01 \div 0.13$), while higher peaks are found for each frequency f_j across the three scenarios s_i (i.e., $\sigma_{\varepsilon_r} = 0.11 \div 0.19$). It is then reasonable to argue that a variation in the arrangement of the clean ballast stones in dry conditions, as reproduced here by each scenario s_i, may affect permittivity values more than using multiple frequencies, within those available herein. Concerning the impact brought by the use of several frequencies across the three scenarios investigated (i.e., the trend of the average permittivity $\overline{\varepsilon_r}$ in the fourth grey column of Fig. 5), it can be broadly argued that the higher the central frequency of investigation, the higher the value of permittivity. In line with this and according to the processed data alone, $\overline{\varepsilon_r}$ ranges from 3.69 (i.e., 1000 MHz) up to 3.87 (i.e., 2000 MHz (NA)). With regard to the effects on ε_r of the data processing scheme applied, it is worth noting a slight increase in the average permittivity values $\overline{\varepsilon_r}$ of the processed data, in both the amounts observed across the various scenarios s_i (same frequency: $\overline{\Delta\varepsilon_{\text{r proc-raw}}} = 0.2 \div 0.6$; i.e., fourth grey column in Fig. 5) and frequencies f_j (same scenario: $\overline{\Delta\varepsilon_{\text{r proc-raw}}} = 0.3 \div 0.8$; i.e., last two grey rows in Fig. 5) used. In this regard, Fig. 6 shows the incidences of residuals between processed and raw data for any combination of f_j and s_i. Such data confirm that the processing scheme returns mostly higher dielectrics, whose incidence of residuals does not exceed 3%.

In Fig. 7, the processed values of ε_r with the TDSP technique are compared with the corresponding dielectrics achieved with the SRM approach. It is clear how the former method returns broadly lower values of ε_r with respect to the peak-to-peak estimates, and appears to be unsuitable for characterizing clean basalt stones in dry conditions across the

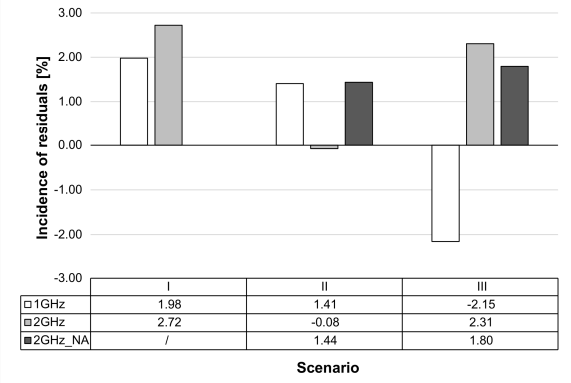

	I	II	III
1GHz	1.98	1.41	-2.15
2GHz	2.72	-0.08	2.31
2GHz_NA	/	1.44	1.80

Fig. 6. Incidence of residuals between processed and raw data

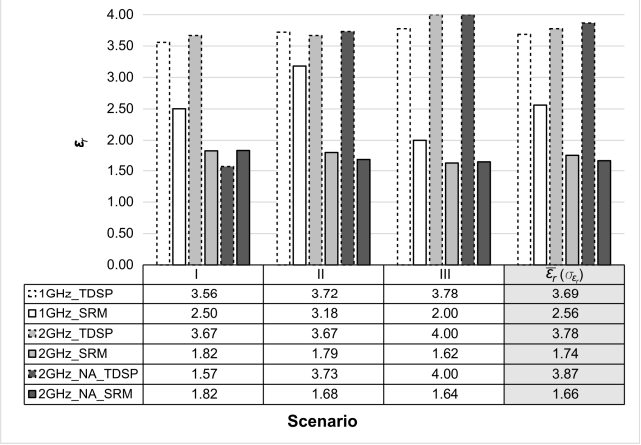

	I	II	III	$\overline{\varepsilon_r(\alpha_k)}$
1GHz_TDSP	3.56	3.72	3.78	3.69
1GHz_SRM	2.50	3.18	2.00	2.56
2GHz_TDSP	3.67	3.67	4.00	3.78
2GHz_SRM	1.82	1.79	1.62	1.74
2GHz_NA_TDSP	1.57	3.73	4.00	3.87
2GHz_NA_SRM	1.82	1.68	1.64	1.66

Fig. 7. Relative dielectric permittivity estimates (processed) for the 1000 MHz, 2000 MHz, and 2000 MHz (NA) central-frequency acquisitions using the TDSP and the SRM methods

thickness defined by the investigation domain. This may reasonably be due to a higher sensitivity of the SRM towards the roughness in the grain size of the ballast at the interface between the air and the ballast system. This is confirmed by the highest permittivity estimates reached with the SRM in the case of the 1000 MHz central frequency (i.e., $\overline{\varepsilon_{r\,1GHz}}$ = 2.56 against $\overline{\varepsilon_{r\,2GHz}}$ = 1.74 and $\overline{\varepsilon_{r\,2GHz\_NA}}$ = 1.66), whereby the relevant wavelength is higher than those of the 2000 MHz GPR systems.

VI. Conclusions

In this paper, ballast material typically employed in rail track bed construction has been characterized. Laboratory tests have been carried out over a methacrylate tank, which was filled up and emptied with basalt stones several times, thereby providing different scenarios of ballast stone arrangement. Four GPR systems and five different antenna frequencies have been used. The impacts brought to the estimate of relative dielectric permittivity by the combination of several i) radar systems, ii) frequencies of investigation, iii) scenarios of stone arrangement, and iv) methods of dielectric permittivity estimate, have been analyzed.

The results have shown that ground-coupled GPR systems with 600 MHz and 1600 MHz central frequencies of investigation return values of dielectric permittivity higher than those of relevant studies in the literature, and likely ringing effects may be the cause of this. On the contrary, values in line with the literature have been found for air-coupled GPRs. A strong impact on the permittivity is brought by the variation of ballast stone arrangements using the same frequency, while minor variations are encountered when using multiple frequencies within the same scenario. In addition, higher permittivity estimates are found for higher-frequency investigations once the processing scheme discussed above is performed. Finally, the use of the SRM turned out to be not suitable for characterizing ballast material due to both its coarse grain size and the depth of the domain of investigation in this study.

Acknowledgments

The authors express their thanks to Mr. Spartaco Cera, from Roma Tre University, for the assistance during the surveys. Special thanks to IDS Ingegneria dei Sistemi S.p.A. for supplying a part of the radar systems, and Clax Italia s.r.l. for manufacturing the methacrylate tank. This work has also benefited from the network activities carried out within the EU funded COST Action TU1208 “Civil Engineering Applications of Ground Penetrating Radar.”

References

[1] M. R. Clark, R. Gillespie, T. Kemp, D. M. McCann, and M. C. Forde, “Electromagnetic properties of railway ballast,” NDT & E International, vol. 34, pp. 305–311, 2001.

[2] R. Roberts, I. Al-Qadi, E. Tutumluer, J. Boyle, and T. R. Sussmann, “Advances in Railroad Ballast Evaluation Using 2 GHz Horn Antennas”, in Proc. 11th International Conference on Ground Penetrating Radar, Columbus, OH., USA, 2006.

[3] F. Tosti and L. Pajewski, “Applications of radar systems in Planetary Sciences: an overview,” Chapt. 15 - Civil Engineering Applications of GPR, Springer Trans. in Civ. and Environm. Eng. Book Series, pp. 361–371, 2015.

[4] A. Benedetto and L. Pajewski, Civil Engineering Applications of Ground Penetrating Radar. Springer Transactions in Civil and Environmental Engineering Book Series, 2015.

[5] A. K. Benson, “Applications of ground penetrating radar in assessing some geological hazards: examples of groundwater contamination, faults, cavities,” Journal of Applied Geophysics, vol. 33 (1-3), pp. 177–193, 2001.

[6] D. Goodman, “Ground-penetrating radar simulation in engineering and archaeology,” Geophysics, vol. 59 (2), pp. 224-232, 1994.

[7] J. J. Schultz, M. E. Collins and A. B. Falsetti, “Sequential monitoring of burials containing large pig cadavers using ground-penetrating radar,”J. Foren. Sci.,51 (3),607-616, 2006.

[8] D.J. Daniels, Ground Penetrating Radar, 2nd Edition. London, U.K.: The Inst. Electrical Eng., 2004.

[9] T. Saarenketo and T. Scullion, “Road Evaluation with Ground Penetrating Radar,” J. Appl Geophys., 43, pp. 119–138, 2000.

[10] I. L. Al-Qadi and S. Lahouar, “Use of GPR for thickness measurement and quality control of flexible pavements,” J. Ass. Asph. Paving Technologists vol. 73, pp. 501–528, 2004.

[11] C. Fauchard, X. Dérobert, J. Cariou, and P. Côte, “GPR performances for thickness calibration on road test sites,” NDT and E International, vol. 36 (2), pp. 67-75, 2003.

[12] A. Loizos and C. Plati, "Accuracy of pavement thicknesses estimation using different ground penetrating radar analysis approaches," NDT & E International, vol. 40 (2), pp. 147-157, 2007.

[13] F. Tosti, S. Adabi, L. Pajewski, G. Schettini, and A. Benedetto, "Large-scale analysis of dielectric and mechanical properties of pavement using GPR and LFWD," in Proc. 15th International Conference of Ground Penetrating Radar (GPR 2014), Brussels, Belgium, Jun. – Jul. 2014, art. no. 6970551, pp. 868-873.

[14] A. Benedetto and F. Tosti, "Inferring bearing ratio of unbound materials from dielectric properties using GPR: the case of Runaway Safety Areas," in Proc. Airfield and Highway Pavement 2013: Sustainable and Efficient Pavements, Los Angeles, USA, June 2013, pp. 1336–1347.

[15] C. Patriarca, F. Tosti, C. Velds, A. Benedetto, S. Lambot, and E. C. Slob, "Frequency dependent electric properties of homogeneous multi-phase lossy media in the ground-penetrating radar frequency range," Journal of Applied Geophysics, vol. 1 (97), pp. 81–88, 2013.

[16] F. Tosti, A. Benedetto, L. Bianchini Ciampoli, S. Lambot, C. Patriarca, and E. C. Slob, "GPR analysis of clayey soil behaviour in unsaturated conditions for pavement engineering and geoscience applications," Near Surface Geophysics, vol. 14 (2), pp. 127-144, 2016.

[17] I. L. Al-Qadi and S. Lahouar, "Measuring rebar cover depth in rigid pavements with ground-penetrating radar," Transportation Research Record, vol. 1907, pp. 81-85, 2005.

[18] A. Benedetto, F. Tosti, B. Ortuani, M. Giudici, and M. Mele, "Mapping the spatial variation of soil moisture at the large scale using GPR for pavement applications," Near Surface Geophysics, vol. 13 (3), pp. 269-278, 2005.

[19] F. Benedetto, F. Tosti, "GPR spectral analysis for clay content evaluation by the frequency shift method," Journal of Applied Geophysics, vol. 1 (97), pp. 89–96, 2013.

[20] A. S. Jørgensen, F. Andreasen, "Mapping of permafrost surface using ground-penetrating radar at Kangerlussuaq Airport, western Greenland," Cold Regions Science and Technology, vol. 48 (1), pp. 64–72, 2007.

[21] A. Benedetto, G. Manacorda, A. Simi, and F. Tosti, "Novel perspectives in bridge inspections using GPR," Nondestructive Testing Evaluation, vol. 27(3), pp. 239–251, 2012.

[22] A. M. Alani, M. Aboutalebi, and G. Kilic, "Applications of ground penetrating radar (GPR) in bridge deck monitoring and assessment", Journal of Applied Geophysics, vol. 97, pp. 45-54, 2013.

[23] A. M. Alani and K. Banks, "Applications of ground penetrating radar in the Medway Tunnel - Inspection of structural joints", in Proc. 15th International Conference of Ground Penetrating Radar (GPR 2014), Brussels, Belgium, Jun. – Jul. 2014, art. no. 6970466, pp. 461–464.

[24] R. Roberts, A. Schutz, I. L. Al-Qadi, and E. Tutumluer, "Characterizing railroad ballast using GPR: recent experiences in the United States", in Proc. of the 2007 4th International Workshop on Advanced Ground Penetrating Radar (IWAGPR 2007), Naples, Italy, 2007, pp. 295–299.

[25] Railway Track and Structures Magazine, June 1985.

[26] J. Hugenschmidt, "Railway track inspection using GPR", J. of Applied Geophysics, vol. 43 (2-4), pp. 147–155, 2000.

[27] G. R. Olhoeft and E. T. Selig, "Ground penetrating radar evaluation of railroad track substructure conditions", in Proc. 9th International Conference on Ground Penetrating Radar (GPR 2002), Santa Barbara, USA, Apr. – May 2002.

[28] Z. Leng and I. L. Al-Qadi, "Railroad ballast evaluation using ground-penetrating radar," Transportation Research Record: Journal of the TRB, no. 2159, pp. 110–1117, 2010.

[29] T. R. Sussmann, K. R. O'Hara, and E. T. Selig, "Development of material properties for railway application of ground penetrating radar", in Proc. of the Society of Photo-Optical Instrumentation Engineers (SPIE), vol. 4758, 2002.

[30] F. De Chiara, "Improvement of railway track diagnosis using ground penetrating radar," PhD Thesis, 2014.

[31] F. Tosti, C. Patriarca, E. Slob, A. Benedetto, and S. Lambot, "Clay content evaluation in soils through GPR signal processing," Journal of Applied Geophysics, vol. 97, pp. 69-80, 2013.

[32] J. Redman, J. Davis, L. Galagedara, and G. Parkin, "Field studies of GPR air launched surface reflectivity measurements of soil water content", in Proc. of the 9th International Conference on Ground Penetrating Radar (GPR 2002), Santa Barbara, California, USA, 2002, art. no. 4758, pp. 156-161.

[33] A. P. Annan, 1999, Practical processing of GPR data, Sensors and Software Inc., 1999.

[34] H. Jol, Ground Penetrating Radar, Ed. Elsevier, 2009.

[35] ASTM D6087-08, "Standard Test Method for Evaluating Asphalt-Covered Concrete Bridge Decks Using Ground Penetrating Radar," ASTM International, West Conshohocken, PA, 2008.

[36] L. Pajewski, F. Tosti, and W. Kusayanagi, "Antennas for GPR Systems," Chapter 2 - Civil Engineering Applications of Ground Penetrating Radar, Springer Transactions in Civil and Environmental Engineering Book Series, 41–67, 2015.

[37] EN 13450:2002/AC:2004, "Aggregates for railway ballast," Europ. Comm. for Standardization, 2004.

[38] EN 933-1:2012, "Tests for geometrical properties of aggregates - Part 1: Determination of particle size distribution -Sieving method," Europ. Comm. for Standardization, 2012.

[39] EN 1097-2:2010, "Tests for mechanical and physical properties of aggregates - Part 2: Methods for the determination of resistance to fragmentation," Europ. Comm. for Standardization, 2010.

[40] CEN ISO/TS 17892-1:2014, "Geotechnical investigation and testing - Laboratory testing of soil - Part 1: Determination of water content (ISO 17892-1:2014)," Europ. Comm. for Standardization, 2014.

[41] EN1097-6:2013,"Tests for mechanical and physical properties of aggregates-Part 6:Determination of particle density and water absorption," Europ Comm for Stand, 2013.

[42] EN 1097-3:1998, "Tests for mechanical and physical properties of aggregates - Part 3: Determination of loose bulk density and voids," Europ. Comm. for Standardization, 1998.

[43] I. L. Al-Qadi, W. Xie, and R. Roberts, "Scattering analysis of ground-penetrating radar data to quantify railroad ballast contamination,"NDT&E Int., vol. 41, pp. 441-447, 2008.

[44] S. Lambot, M. Antoine, M. Vanclooster, and E. C. Slob, "Effect of soil roughness on the inversion of off-ground monostatic GPR signal for noninvasive quantification of soil properties," Water Resources Research, vol. 42 (3), 20